Soil Dynamics and Earthquake Engineering xxx (xxxx) xxx–xxx

Contents lists available at ScienceDirect

Soil Dynamics and Earthquake Engineering

journal homepage: www.elsevier.com/locate/soildyn

Seismic site classification

Ramón Verdugo

CMGI, Virginia Opazo 48, Santiago, Chile

ARTICLE INFO

Keywords:
Performance based design
Site effect
Shear wave velocity
Spectral ratio

ABSTRACT

The economic losses left by large recent earthquakes are still considerable, and modern society is wanting not only life protection; it is also demanding that buildings can be immediately occupied after a strong earthquake. The performance-based seismic design allows engineers to design structures with a desired seismic performance for a specified level of hazard. This requires a high standard in the different items involved in the seismic design. One of the key factors is associated with the seismic loads, which are strongly dependent on the local ground conditions. Accordingly, an alternative seismic site classification is proposed, which is based on two dynamic parameters of the ground: the equivalent shear wave velocity, $V_{S30\text{-}E}$, that reproduces the dynamic lateral stiffness of the upper 30 m of the ground, and the predominant period of the site, which is proposed to be estimated applying the H/V spectral ratio of ambient vibration measurements. All the details of this site classification are explained in the paper.

1. Introduction

In spite of the tremendous advances in the field of earthquake engineering, economic losses generated by recent earthquakes are still considerable, far from any socio-economically satisfactory standard. An important part of these losses is attributed to the severe damages suffered by buildings (residential, commercial, industrial, governmental, educational, cultural, hospital, etc.), infrastructure and structures of the production sector. In Table 1 the estimated direct economic losses of the latest earthquakes are presented (Data from USGS[1], Kajitani et al. [2], Horspool et al. [3], Aon Benfield [4] and Senplades [5]). It can be observed that in the particular case of Tohoku Earthquake, the cost is substantially high due to the damages caused by the tsunami. In any case, modern society is wanting not only life protection; it demands that buildings can be occupied and function following a strong earthquake. This also means that water, electricity, gas, and other services have to be operational as well. Therefore, the challenge is to reduce the tremendous economic impact that earthquakes still have on society, and accordingly, resilience and reliability of structures is an important issue [6].

According to FEMA [7], one of the most promising tools that can be used to reduce the damage and losses resulting from an earthquake, or other similar disaster, is the performance-based seismic design (PBSD). The philosophy of this design methodology is to accomplish a reliable structure design meeting performance objectives [8]. Historically, seismic design has focused on providing resistance to the structural components of the structures. However, it is well recognized that this approach by itself does not guarantee successful seismic behavior of the structure. For example, it is well known that it is inadequate to provide higher resistance to the beams than to the columns in a frame structure; under severe seismic loadings a better response is expected if plastic hinges are developed in the beams rather than in the columns. This example suggests that, conceptually, an appropriate seismic design should identify the overall performance of the structure when subjected to strong earthquakes. Accordingly, the seismic design has moved from resistance criteria to performance objectives that have to be satisfied by the structures during and after earthquakes.

PBSD has the advantage of considering both the level of ground shaking and the associated level of performance. This means that for different levels of shaking considered as input motion, different target performance levels can be specified or requested. In the framework of PBSD, it is apparent that the proper estimation of the seismic loads to which the structure will be subjected turns out to be a fundamental issue in the analysis. This is commonly done using modal spectral analysis, which requires a spectrum associated with the considered seismic action. Besides the seismic hazard level, the considered spectrum is strongly dependent of the ground conditions, or geotechnical-geological characteristics of the site. Different local site conditions may generate quite different spectral shapes, which may change drastically the seismic loads applied on the analyzed structure.

According to the philosophy of PBSD explained above, it is essential to keep in mind that PBSD requires that each of the steps associated with the analyses be performed with the lowest level of uncertainty that the profession may guarantee. In this respect, it is evident that the

E-mail address: rverdugo@cmgi.cl.

https://doi.org/10.1016/j.soildyn.2018.04.045
Received 12 September 2017; Received in revised form 6 April 2018; Accepted 25 April 2018

Table 1
Economic loss of recent earthquakes.

Earthquake	Dater	Mw	Direct Loss (billion US$)
Maule, Chile	February 2010	8.8	30
Tohoku, Japan	March 2011	9.0	211
Christchurch, NZ	Febru. 2011	6.3	40
Nepal	April 2015	7.8	10
Muisne, Ecuador	April 2016	7.8	3

assessment of the seismic loads to be applied to the analyzed structures is a fundamental issue. Nonetheless, this is probably one of the weakest points involved in the actual application of PBSD. Besides the seismologic study for establishing the earthquake characteristics of the different seismic hazard levels and the engineering decision to adopt a particular seismic scenario, the resulting seismic loads are strongly dependent on the local geological-geotechnical conditions of the ground where the structure will be located [9,10]. This phenomenon is commonly referred to as a site effect. Even though this is a well-known fact, the seismic site classifications adopted by different seismic provisions suffer from a rather simplistic methodology that in many cases can wrongly estimate the design spectra, and consequently, the acting seismic forces can be seriously underestimated. If this happens, the PBSD loses all its capability for predicting the structure response under different seismic hazard levels. Thus, the site effect and therefore, the site classification are important issues that are addressed in this paper and an alternative procedure is proposed.

2. Empirical evidence of site effect

Under large earthquakes it has been observed that, in general, structures placed on rock outcrops and stiff soil deposits consisting of dense granular materials behave well with no damage or only with some minor negative seismic effects. Conversely, when the soil conditions are associated with soft materials (as for example, saturated clayey or deep deposits of sandy soils), it is common the occurrence of severe damages, and even the collapse of structures when subjected to strong earthquakes [11–14]. A remarkable case of amplification is the one observed during the 1985 Mexico City earthquake of Magnitude 8.1, where the shaking was amplified by a factor of 20, or even more, on sites consisting of deep soil deposits of soft fines materials [15,16]. On the other hand, rock outcrops and stiff soil deposits have shown a significant reduction in the shaking intensity [11–14].

An interesting experience that clearly shows the site effect took place during the 1906 Valparaiso Earthquake of Magnitude, Mw = 8.2. This strong ground motion occurred approximately 4 months after the San Francisco Earthquake, where similar site effects were observed [17]. At the time of this earthquake (before the Panama Canal), Valparaiso was an important port due to its location in the south coast of the Pacific Ocean, with a significant amount of buildings and infrastructures, which were similar in terms of engineering materials, construction and design. In this context, the concentration of damages can be directly attributed to the ground conditions.

Fig. 1 shows the general geology of Valparaíso, which basically consists of a massive rock outcrop of the Coastal Range and a rather small plane area consisting mainly of medium to dense sandy soils. A borehole performed near to the National Congress (Fig. 2) found bedrock at a depth of 57 m. Therefore, the ground conditions can be separated in only two main units: rock outcrop (or shallow bedrock) and a soil deposit of medium depth consisting of sandy materials.

Severe destruction of buildings located in the soil deposit was reported as shown the photo of Fig. 3. Two emblematic building, Teatro Victoria (built in 1886) and Iglesia de la Merced (built in 1893), collapsed during the earthquake, as shown in the photos of Fig. 4 [19]. On the other hand, some buildings underwent minor damages during the

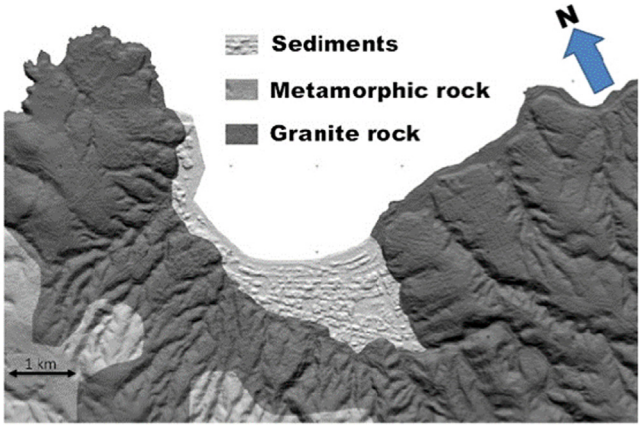

Fig. 1. General geology of Valparaiso. (with slight modification from Indirli et al. [18]).

Fig. 2. Location of emblematic buildings that collapsed during the 1906 Earthquake (red dots), and buildings that exist even today (blue dots). (For interpretation of the references to color in this figure legend, the reader is referred to the web version of this article.).

Fig. 3. Total destruction in the area of ground consisting of a sandy soil deposit (intersection of Blanco and Edwards streets).

1906 Valparaiso Earthquake, as Aduana and Palacio Lyon. The Aduana building is located on rock outcrop and Palacio Lyon is quite close to the rock outcrop, so the bedrock is expected a few meters below this building, as indicated in Fig. 2. These two historical buildings still exist today as shown in the photos of Fig. 5, which means that they have also responded appropriately to the series of shakes that occurred later, especially during the 1985 (Mw = 8.0) and 2010 (Mw = 8.8) earthquakes.

Henriquez [20] and Montessus de Ballore [11] concluded that

Fig. 4. De la Merced Church (on top) and Victoria Theater (below) before and after de 1906 Earthquake.

Fig. 6. Hilly area with undamaged buildings.

geological conditions were fundamental in the observed damage. They reported that buildings placed on soil deposits suffered heavy damage, while structures placed on hills (rock outcrops) experienced no damage, or it was negligible. This is confirmed in the photo of Fig. 6, which shows refugees in the hilly area and the undamaged buildings that amazingly remained in this zone of rock outcrop.

3. Seismic site characterization

Analyzing more than 100 acceleration records with PGA greater than 0.05 g, Seed and co-workers [21] proposed normalized spectral forms considering the site-dependent ground motion characteristics. The mean spectra categories defined by this pioneer work for different site conditions are shown in Fig. 7. The differences of these spectral shapes are evident, being very significant for periods greater than 0.5 s, where soil deposits consisting of soft to medium clays and sands present the higher spectral amplification. Conversely, for periods below 0.4 s, the higher spectral amplification is observed in deposits consisting of stiffer soils. These results were also reproduced by other studies [22], and then incorporated in the ATC 1978, using idealized spectral shapes considering three site conditions, as shown in Fig. 8, where the concept of Site Class, or Soil Type, for grouping sites with similar geotechnical-geological conditions was introduced.

Each soil type would develop the same seismic amplification, which is assigned through a specific design response spectrum. Site Class is determined based on the properties of the soils existing in the top 30 m of the ground. However, it is apparent that from a seismic point of view,

Fig. 5. Aduana (left) and Palacio Lyon (right), examples of buildings founded on bedrock that resulted with minor damages after the 1906 Earthquake, and today are still in usage.

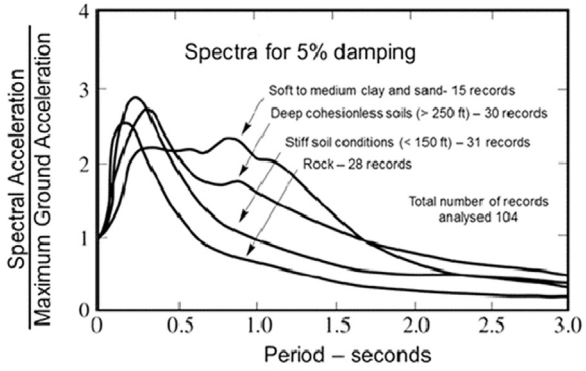

Fig. 7. Average normalized acceleration spectra for different site conditions [21].

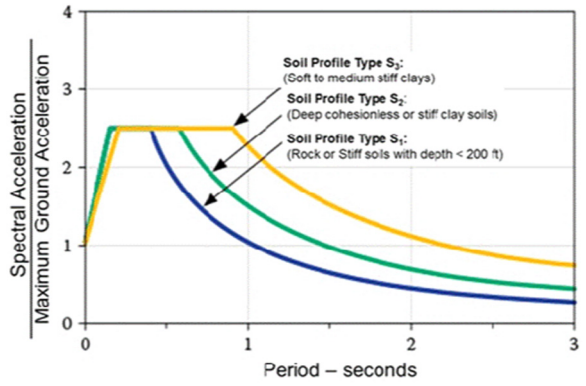

Fig. 8. Spectral shapes proposed by ATC 3 (1978) for three different Soil Types.

deep soil deposits cannot be characterized considering only the upper 30 m of the ground. This is revisited later.

An attempt to classify the geotechnical site conditions unambiguously was introduced by Borcherdt and Glassmoyer [23] and Borcherdt [24], by means of the representative shear wave velocity, V_{S30}, of the upper 30 m of the soil profile. The value of V_{S30} is such that reproduces the vertical travel time of the shear wave propagating throughout the top 30 m of the ground. Accordingly, the expression for its evaluation is:

$$V_{S\,30} = \frac{\sum_{i=1}^{n} h_i}{\sum_{i=1}^{n} h_i / V_{S\,i}} \tag{1}$$

Where, n corresponds to the number of layers identified in the upper 30 m of the ground. The terms hi and Vsi represent the thickness and shear wave velocity, respectively, of the layer i.

The decision of adopting a depth of 30 m was somewhat arbitrary and is mainly associated with practical reasons; it corresponds to the typical exploration depth of geotechnical boreholes. Although in some soil profiles this parameter may lead to incorrect assessments of the site amplification, most of the code provisions for civil structures have adopted it as the main parameter for site classification.

The International Building Codes (IBC) and ASCE7 [25] have established Site Class A to F (Table 2). Site Class A, hard rock, associated with a shear wave velocity, $V_{S30} > 1500$ m/s, corresponds to the most competent geotechnical material. This type of rock could be found to the east of Rocky Mountains. In regions of high seismicity, this type of rock is unusual, and therefore, other seismic codes do not consider this type of rock. In contrast, Site Class B, defined as a rock with $V_{S30} > 750$ m/s, is a common rock outcrop in seismic regions. At the other extreme, site class F corresponds to sites with special soil conditions such as liquefiable soils, sensitive clays, highly organic clays, very high plasticity clays and very thick soft clays. As a result, Site Class F

Table 2
Site classification ASCE7–10.

Site class	$\overline{V_{S30}}$ (m/s)	$\overline{N}$ or $\overline{N_{ch}}$	$\overline{S_u}$ (kPa)
A. Hard rock	> 1500	NA	NA
B. Rock	750–1500	NA	NA
C. Very dense soil and soft rock	360–750	> 50	> 96
D. Stiff soil	180–360	15–50	48–96
E. Soft clay soil (*)	< 180	< 15	< 48
F. Requires site response analysis			

(1 ft/s = 0.3048 m/s; 1 lb/ft^2 = 0.0479 kN/m^2).
(*): Any profile with more than 3 m of soil having the following characteristics: Plasticity index PI > 20; Moisture content w ≥ 40%; Undrained shear strength, S_u < 24 kPa.

requires special analyses. It is important to observe that although the main parameter to classify a site is V_{S30}, strength parameters such as penetration resistance (N-SPT) and undrained shear strength (Su), of the upper 30 m of the ground, can also be used.

Conceptually, the seismic amplification phenomenon, like any other dynamic behavior that is far from any type failure, requires for its analysis material parameters associated with stiffness, damping and mass. Therefore, strength parameters are not the most suitable ones for site characterization, and their use should only be complementary. It is interesting to note that the ASCE7–16 gives an option for those situations with a lack of information: "…Where the soil properties are not known in sufficient detail to determine the site class, Site Class D, subject to the requirements of shall be used unless the authority having jurisdiction or geotechnical data determine that Site Class E or F soils are present at the site.". This option seems rational and useful when the site is somehow isolated (far from urban areas) and the projected structures are rather small, so any potential overdesign does not affect significantly the cost of the project. However, in normal conditions of site investigation, this alternative seems should not be available.

Another valuable code is the Eurocode 8 (EC8) [26], where five Ground Types, identified as A, B, C, D and E have been established (Table 3). Each Ground Type is defined according to the resulting value of V_{S30}. However, when shear wave velocities are not available, resistance parameters such as N-SPT and Su may be used to select the corresponding Ground Type. It is considered important to comment again that resistance parameters are not the best option to characterize a site from its expected dynamic response.

In the EC8, the Ground Type A represents rock outcrops with $V_{S30} > 800$ m/s, which is similar to Site Class B in the ASCE7–10. In particular, the Ground Type E is introduced, which is defined as a surface alluvium material with $V_S < 360$ m/s and a thickness less than 20 m, underlain by rock ($V_S > 800$ m/s). This singular condition is associated with high impedance ratio that is expected to amplify the seismic response. Similar to IBC and ASCE7, the EC8 has defined singular Ground Types (S1 and S2), which basically consist of soil deposits that require special analyses, for example, fines soils with high plasticity and high water content, liquefiable soils and sensitive clays.

Following similar concepts, the Chilean code DS-61 [27] basically defines six Soil Types identified from A to E according to the shear wave velocity of the upper 30 m, V_{S30} (Table 4). This code requests as primary parameter V_{S30}, and as a complement the N-SPT for sandy soils and Su for fines soils. Additionally to the five Soil Types, the Chilean code has grouped as Site Type F all those soil deposits considered special or unique, for example, liquefiable soil, organics, fines soils of high plasticity and highly sensitive soils, etc. Accordingly, these soils (Soil Type F) require special dynamic analysis.

These three seismic codes (ASCE7–10, EC8 and DS-61) establish geological-geotechnical conditions of the upper 30 m of the ground in order to group the sites with similar expected seismic response. The identification of each site class according to V_{S30} is summarized in

Table 3
Ground Types Eurocode 8.

Ground Type	Stratigraphicprofile	V_{S30} (m/s)	N_{SPT}	S_U (kPa)
A	Rock or other rock-like geological formation.	> 800	–	–
B	Deposits of very dense sand, gravel, or very stiff clay, at least several tens of meters in thickness.	360–800	> 50	> 250
C	Deep deposits of dense or medium-dense sand, gravel or stiff clay with thickness from several tens to many hundreds of meters.	180–360	15–50	70–250
D	Deposits of loose-to-medium cohesionless soil, or of predominantly soft-to-firm cohesive soil.	< 180	< 15	< 70
E	A soil profile consisting of a surface alluvium layer with V_S values of type C or D and thickness varying between 5 and 20 m, underlain by stiffer material with V_S > 800 m/s.			
S_1	Deposits consisting, or containing a layer at least 10 m thick, of soft clays/silts with a high plasticity index (PI > 40) and high water content.	< 100	–	10–20
S_2	Deposits of liquefiable soils, sensitive clays, or any other soil profile not included in types A, E, S_1.			

Table 4
Soil Types of Chilean Code, DS-61.

	Soil Type	V_{S30} (m/s)	RQD (%)	q_u (MPa)	N_1	S_U (MPa)
A	Rock, cemented soils	≥ 900	≥ 50	≥ 10	–	
B	Soft or fractured rock, very dense soils	≥ 500		≥ 0.4	≥ 50	
C	Dense, firm soils	≥ 350		≥ 0.3	≥ 40	
D	Medium-dense or medium-firm soils	≥ 180			≥ 30	≥ 0.05
E	Soils of medium consistency	< 180			≥ 20	< 0.05
F	Special soils	–				

N_1: Normalized N-SPT at 1 kg/cm^2; q_u: Unconfined strength.

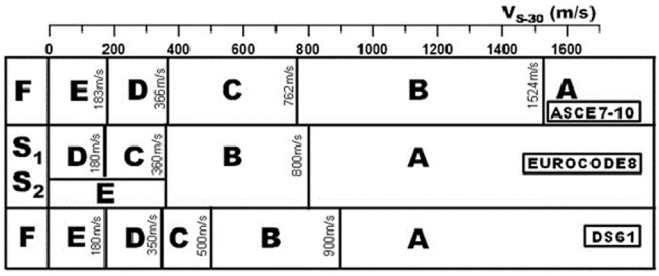

Fig. 9. Boundaries of Soil Types in terms of V_{S30}.

Fig. 9. It can be observed that these three codes use similar values of V_{S30} to separate the different Soil Type, or Site Classes. The exception is the Soil Type C defined in the Chilean code that was introduced to generate a smoother transition from very dense granular material to medium dense sands and stiff clays. Another difference is the frontier between Soil Type A (rock and cemented soils) and Soil Type B (very dense soils) defined in the Chilean code, which is stablished at V_{S30} = 900 m/s, this is because to the west of Los Andes Range there are several non-cemented dense gravelly soil deposits with shear wave velocity in the order of 800 m/s.

The above-described methods to assess the site classification present an inherent weakness; they rest on the properties of the top 30 m of the ground, neglecting the effects of both the properties of the soils below a depth of 30 m and the total depth of the soil layers.

On the other hand, the Japanese provisions for seismic soil classification consider only three site conditions, identified as soil profile types I, II, and III, which are basically representing hard, medium and soft soil deposits. In particular, the Highway Bridge Design Code considers the ground period, T_G, which is calculated as follows:

$$T_G = 4\sum_{i=1}^{n}\frac{h_i}{V_{S\,i}} \tag{2}$$

Where, i represents the i-soil layer defined from the ground surface down to the engineering bedrock, and hi and $V_{S\ i}$ correspond to its respective thickness and shear wave velocity. The engineering base depends on professional judgement, for instance N-SPT ≥ 50 blows, or shear wave velocity greater than 400 m/s (Towhata [28]). The description and requested values of T_G for each of the Soil Types are indicated in Table 5. The Japanese procedure evaluates a kind of simplified period T_G of the upper part of the ground - above the engineering base – considering the classical expression:

Table 5
Soil Types Japanese Highway Bridge Design.

Soil profile	Groundcharacteristics	T_G (s)
Type I (Hard soil)	Rock, hard sandy gravel or gravel, and other soils mainly consisting of tertiary or older layers.	< 0.2
Type II	Other than Type II or III	0.2–0.6
Type III (Soft soils)	Alluvium mainly consisting of organic, mud, or other soft soils.	> 0.6

$$T_G = \frac{4H}{V_{S-H}} = \frac{4\sum h_i}{\sum h_i/\sum\frac{h_i}{V_{S\,i}}} = 4\sum\frac{h_i}{V_{S\,i}} \tag{3}$$

Where, H represents the total thickness of the soils above of the engineering base, and $V_{S\text{-}H}$ corresponds to the shear wave velocity that reproduces the vertical travel time of the shear wave propagating throughout the soil layers, of total thickness H, encountered above the engineering base.

As can be observed, the Japanese provisions associated with the site classification differ from the previous described methods mainly in its attempt of considering the complete soil deposit introducing the concept of engineering bedrock and also in its simplification of including only three soil profiles. Nevertheless, there exist complex soil deposits consisting of several layers of different materials, in which case this site classification can be considered oversimplified.

It is important to recognize the significant amount of research that has been carried out in relation to the site effect, especially in the last 20 years due to the strong increase in the availability of seismic records of large earthquakes. New classifications systems have been introduced, where additional parameters have been considered, as for example, depth of the soil deposits, depositional age of the soils, type of depositional environment, mean H/V spectral ratio amplitudes across periods, depth to the 1 km/s shear wave velocity, depth to the 2.5 km/s shear wave velocity, fundamental frequency as a V_{S30} proxy, characteristic of the H/V spectral ratio near the spectral peaks [29–35]. In general, the preceding works have assessed both the site classification and the ground-motion prediction equations, however, in the present paper the focus is exclusively in the classification system. In this context, an attempt of introducing parameters that have a clear physical meaning and can be obtained with a reasonable ease, has been performed.

4. Suitable parameters for a seismic site classification

Although there are soil deposits with a thickness equal to or less than 30 m, in general, soil deposits are deeper than 30 m. Therefore, any site classification that by definition only takes into account the soil properties of the top 30 m, most probably would wrongly evaluate the seismic response of the site, especially if soil layers with different properties are present below 30 m. In any case, it is important to realize that for ordinary projects a geotechnical exploration down to the bedrock would not be practical, particularly in deep soil deposit.

In spite of that, it is important to recognize that the upper 30 m of ground also plays a role in the resulting seismic response at the ground surface. For example, the recorded accelerations in the LLolleo downhole array [36] showed systematically that the seismic amplification is developed mainly in the upper 20–30 m of the ground. Therefore, characterization of the upper 30 m of a site also provides valuable information about the amplification phenomenon, but is not sufficient. Accordingly, the main task for improving the current state of site classification is to find a complementary parameter that provides fundamental information of the entire soil deposit (from the surface down to the bedrock), influencing its seismic response at the surface. Additionally, a practical requirement for this parameter is that it must be economically affordable. These requirements are fulfilled by the predominant period of a site, which can be estimated through the measurement of ambient vibrations and calculation of the H/V spectral ratio [37–43]. The H/V spectral ratio (HVSR), also referred to as Nakamura´s method, is broadly used in several European and Asian countries. However, it is not broadly used all around the world. Because of this, empirical evidence to confirm its capability to estimate the predominant period of a site is presented below.

Returning to the characterization of the upper 30 m of the ground and recognizing that site amplification is essentially a dynamic phenomenon, it is considered appropriate to use a stiffness parameter rather than a strength parameter. In this context, the shear wave velocity is a suitable parameter to characterize the top 30 m of a site. However, it is necessary to review the actual effectiveness of V_{S30} in capturing the essence of the dynamic soil response. Because V_{S30} corresponds to the shear wave velocity with the same travel time as the actual upper 30 m of the soil deposit, its value is independent of the sequence of the existing soil layers in the top 30 m. Therefore, V_{S30} does not take into account the order of deposition of the different layers existing in the upper 30 m of a site, which is a fundamental geological-geotechnical condition that seriously affect the seismic site response. Accordingly, another parameter is proposed; the equivalent shear wave velocity ($V_{S30\text{-}E}$) that reproduces the shear stiffness of the top 30 m of the ground, based on the shear wave velocities of the existing layers on the upper 30 m.

Consequently, to characterize a site for an estimation of its expected seismic response at the ground surface, the use of the following two parameters are proposed:

- The equivalent shear wave velocity of the upper 30 m of the site that reproduces the shear stiffness of these upper 30 m.
- The predominant period of the site evaluated through the H/V spectral ratio on ambient vibrations measurements.

The estimation of these parameters and the proposed methodology of how to combine these two parameters for a seismic site classification is presented below.

5. Estimation of the predominant period of a site

Accepting that a soil deposit has a fundamental period of vibration, identified by the maximum amplification of the transfer function (ratio between Fourier spectra of ground surface to bedrock), the question that immediately would arise is whether this predominant period, or frequency, is manifested in the acceleration time history that takes place at the ground surface. From a theoretical point of view, if the input motion at the bedrock brings a broad frequency content, with more or less similar amplitudes, the soil deposits will acts as a filter amplifying its natural frequency, or fundamental period of vibration. This implies that the acceleration time histories recorded at the ground surface should have a response spectrum with a maximum amplification at the fundamental period. However, depending on the seismic source (type of earthquake and path of the seismic waves, among other factors), the input motion that takes place at the bedrock may have more energy in certain particular frequencies and lack of others. Strictly, this means that the frequency content resulting at the ground surface is affected by both the transfer function of the soil deposit and by the frequency content of the seismic source. Nevertheless, large earthquakes are characterized by a broad band of frequencies, and therefore, the natural frequencies of soil deposits should be manifested on the acceleration time histories developed at ground surface. With this in mind, the available acceleration records of two recent large earthquakes - Maule and Illapel - that occurred in Chile are analyzed. Complementary, in the sites where the seismic stations that recorded these earthquakes are located, the HVSR of ambient vibration or micro-tremors were also evaluated. A brief description of Maule and Illapel earthquakes is presented as follows.

Maule Earthquake: It hit the Central-South region of Chile on February 27, 2010 with a Magnitude Mw = 8.8. This earthquake corresponds to a thrust-faulting type event associated with the subduction seismic environment caused by the collision between the Nazca and South American tectonic plates. The rupture zone responsible for this mega event covered a rectangular area of approximately 550 km by 170 km, at an average depth of 35 km. A total number of 36 seismic stations located in the most affected area recorded the acceleration time histories on rock outcrops and soil deposits of different geotechnical characteristics. The maximum PGA recorded on a rock outcrop was 0.32 g in Santa Lucía Hill in Santiago, whereas the maximum PGA recorded on a soil deposit reached a value 0.94 g in Angol city, located close to the south end of the rupture zone. The recorded horizontal peak accelerations are presented in Fig. 10 [44]. The rectangular area enclosed by a broken line corresponds to the rupture zone.

Illapel Earthquake: On September 16, 2015, the Illapel Earthquake, of magnitude Mw = 8.3, hit the Central-Noth region of Chile. The rupture plane occurred at a depth of 23 km, according to the National Seismological Center [45]. The highest horizontal acceleration recorded was 0.83 g (station C110, component E-W). Although this seismic event is of large magnitude and induced considerable peak accelerations, the level of damages were significantly low. This could be explained by the reduced population existing in the affected area, and also, by the good geotechnical conditions of the ground in this area of poor precipitation. The available records with horizontal maximum accelerations equal to or greater than 0.2 g were analyzed, which correspond to eight stations as shown in Table 6.

In the case of Maule Earthquake, the available information of HVSR obtained using ambient vibrations measured near the seismic stations was used to obtain the predominant period of the station sites. However, this information is not available yet in the case of the stations that recorded the Illapel Earthquake. Nevertheless, in these stations, besides the Illapel Earthquakes, several small earthquakes were also recorded, which have been used as micro-tremors to evaluate the HVSR and then the predominant periods of the sites where the stations are located.

The psedo-acceleration response spectra evaluated from the recorded acceleration time histories provide information about the frequency content of the signal, and therefore, it could possible to obtain the predominant period of the sites where the stations are located. Nevertheless, depending on the geotechnical and geological conditions of the site, as well as the seismic source characteristic, it is possible to have spectra with several peaks of similar amplitudes being difficult to

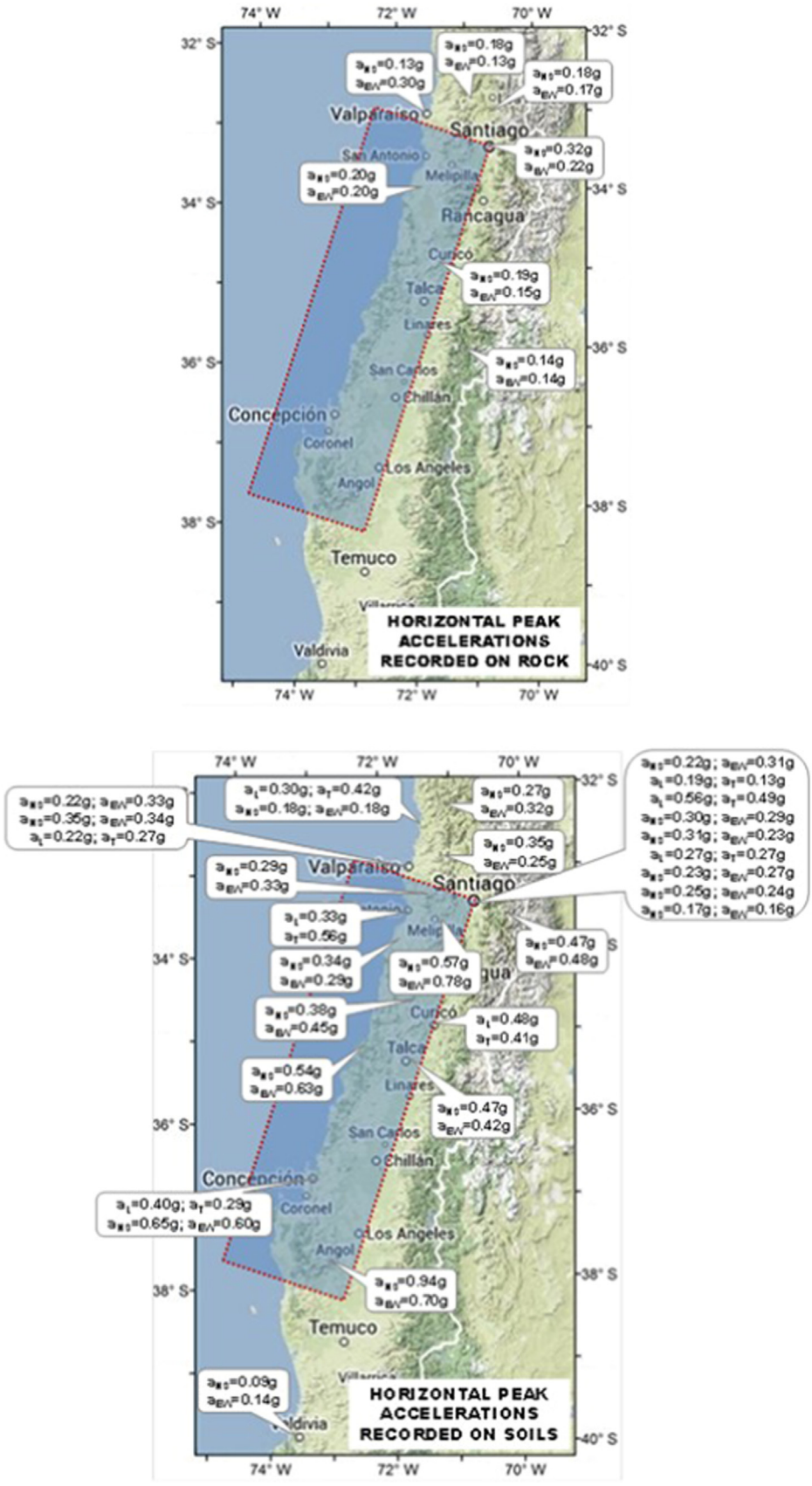

Fig. 10. Horizontal peak acceleration recorded on rock outcrops and soil deposits. 2010 Maule Earthquake.

Table 6
Stations with recorded PGA greater than 0.2 g. Illapel Earthquake of Mw = 8.3.

Station	a_{max} (g) N-S	a_{max} (g) E-W	a_{max} (g) Vert.
C110	0.71	0.83	0.48
C180	0.51	0.48	0.23
C260	0.23	0.36	0.13
C003	0.29	0.35	0.20
G004	0.34	0.24	0.16
C100	0.29	0.31	0.19
C140	0.18	0.30	0.16
C200	0.25	0.26	0.18

identify a predominant period. Thus, a complementary tool to estimate the predominant period from the recorded acceleration time histories is proposed as follows.

The psedo-acceleration response spectrum is built taking the peak acceleration of the response of a single degree of freedom (SDOF) oscillator for each natural frequency or period considered in the spectrum. Instead of using the peak acceleration of each response, it is proposed to evaluate the energy of each response. If the response of a SDOF of frequency ω in terms of acceleration is $a_\omega(t)$, the energy, E_ω, of this response is:

$$E_\omega = \int_0^{tf} [a_\omega(t)]^2 \, dt \tag{3'}$$

Where, t_f is the duration of the acceleration response under analysis.

On the other hand, the expression developed by Arias [46] to establish the intensity of an acceleration time history is:

$$I_A = \frac{\pi}{2g} \int_0^{Tt} [a(t)]^2 \, dt \tag{4}$$

Due to the mathematical similarity between expressions [3] and [4], and considering that the Arias Intensity is a well-known parameter, it is proposed to use the Arias Intensity to evaluate the energy of the acceleration responses of the SDOF of different natural frequencies. With this simple procedure, the Arias Intensity Spectrum is introduced, which is proposed as a complementary method for estimating the frequency of an acceleration time history that present the higher energy, and associated with the predominant frequency.

Fig. 11 shows two examples of the effectiveness of Arias Intensity spectrum for assessing the predominant period of acceleration records. The two stations recorded the Maule Earthquake with peak accelerations greater than 0.5 g. Fig. 11a shows the Arias Spectrum (red line identified as S_{Ia}) and the elastic pseudo-acceleration response spectra (5% of damping) of the two components recorded on Maipu seismic station (black line identified as S_a). As can be seen, the Arias Intensity spectrum shows the same period where the response is clearly amplified, suggesting that this period can be considered as the predominant period of the site. Fig. 11b presents the analysis of Constitucion station. In this case, the response spectra show the maximum amplifications at periods of 0.40 and 0.24 s, for the N-S and E-W components, respectively. However, the Arias Intensity spectra of each component are practically the same, 0.33 and 0.34 s, values that correspond to the predominant period of the site, which is confirmed by the HVSR data.

Consequently, in each site where the Maule Earthquake was recorded, the predominant period was obtained using the information provided by the response spectra and the Arias Intensity spectra. A similar analysis was carried out with the available information of each

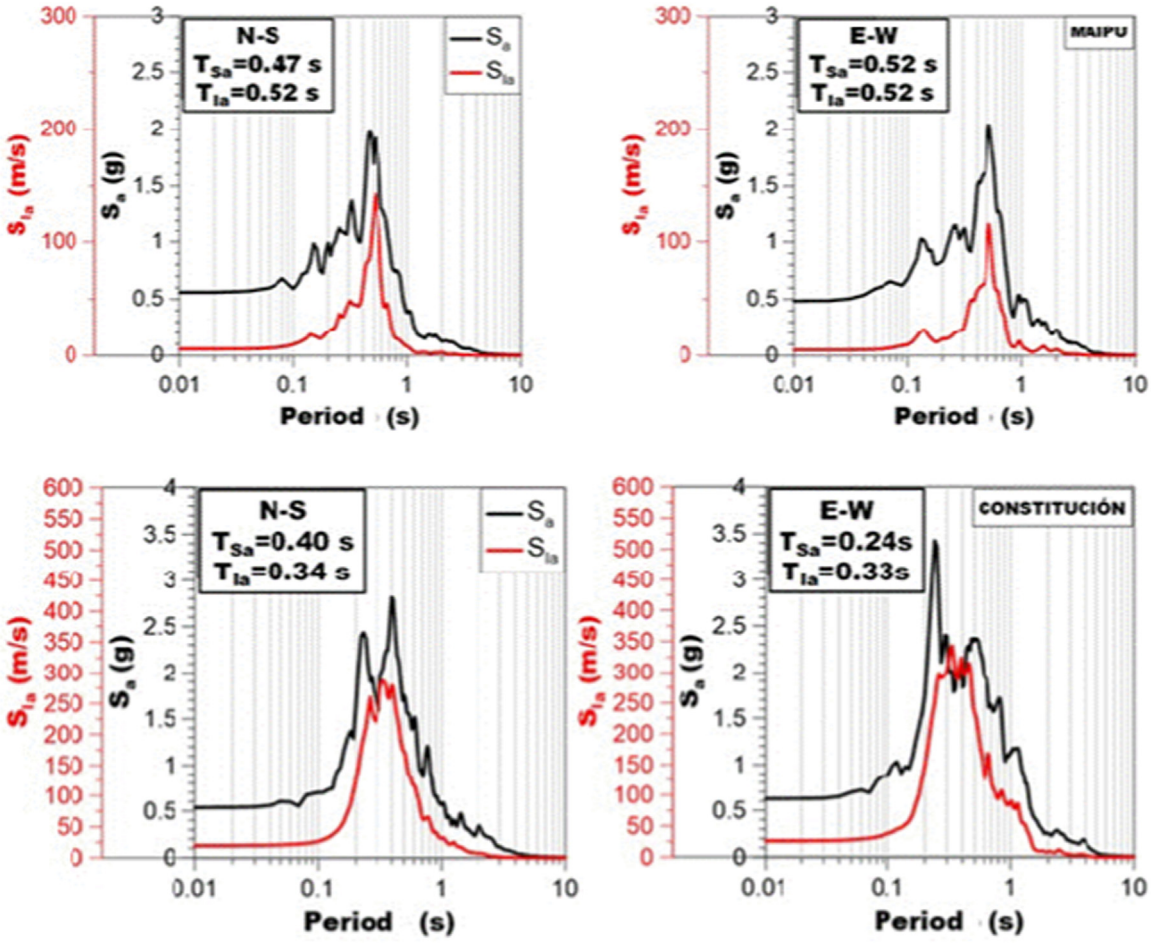

Fig. 11. Response spectra and Arias Intensity spectra of the recorded accelerations at Maipu and Constitucion seismic stations. Maule Earthquake.

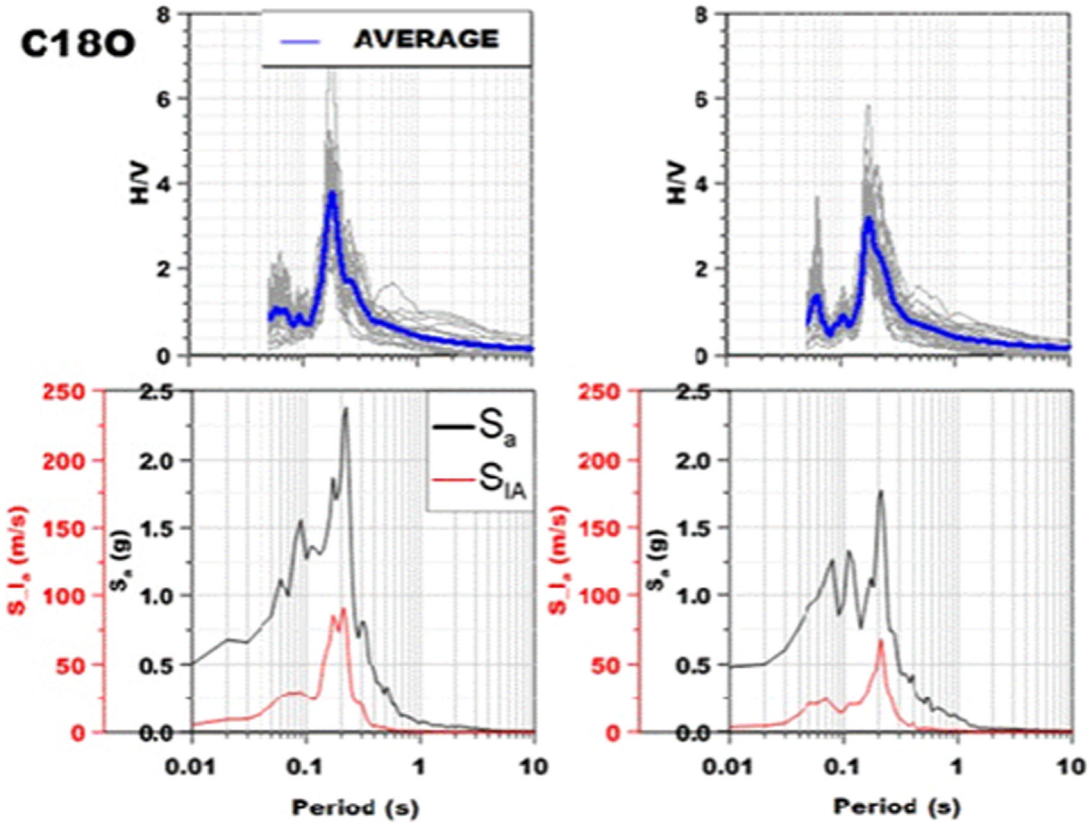

Fig. 12. Station C180. Average HVSR evaluated from micro-tremors recorded in the station (upper plots). Response spectra and Arias Intensity Spectra from Illapel Earthquake record (lower plots).

seismic station that recorded the Illapel Earthquake. As an example, the data obtained at station C180 are presented in Fig. 12, where the HVSR using the micro-tremors recorded in the station and the response spectra and the Arias Intensity spectra of the Illapel Earthquake are plotted.

In Fig. 13 are plotted the predominant periods of the site obtained from the acceleration records against the predominant periods evaluated independently from ambient vibrations (stations of Maule Earthquake) and micro-tremors (stations of Illapel Earthquake). This plot indicates a fairly good agreement between both values, suggesting that the HVSR is a good procedure for evaluating the predominant period of a site, which is coincident with the predominant period estimated from the response spectra and Arias Intensity spectra.

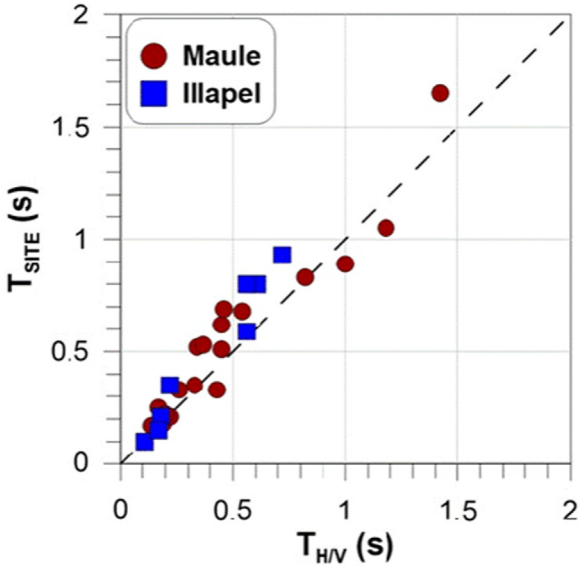

Fig. 13. Predominant period, $T_{H/V}$, evaluated from HVSR, and predominant period, T_{site}, evaluated from the response and Arias Intensity spectra.

It is important to mention that there are a significant number of publications reporting the development of nonlinear site amplification when the shaking is sufficiently strong [47–49]. In this context, it is apparent that the level of strains involved in the HVSR is radically smaller than the strain level induced by strong motions as the case of Maule and Illapel Earthquakes. However, the presented data suggest that the predominant period is not seriously affected by the strain level induced by the shaking. This fact could be explained by the results reported by Choi et al. [50], who concluded that the nonlinearity of amplification factors is significant for sites with $V_{S30} < 180$ m/s, but relatively small for sites with $V_{S30} > 300$ m/s. In this respect, none of the Chilean sites that have been analyzed presented V_{S30} smaller than 210 m/s, and most of them are characterized with a value greater than 350 m/s.

6. Sites with a diffuse predominant period

There are sites that do not show a clear predominant period. These sites are associated with geotechnical conditions of high stiffness, so the impedance between the soil and bedrock is not relevant. Thus, the amplification is low and it takes place in a broad band of frequencies. The acceleration time histories recorded in the station San Jose during the Maule Earthquake show this type of response. Fig. 14 shows a plot of the resulting pseudo-acceleration response spectra of both horizontal components. In particular the E-W component develops several periods where the response is amplified, in the range of 0.1–0.5 s. Although the predominant period could be evaluated using the Arias Intensity

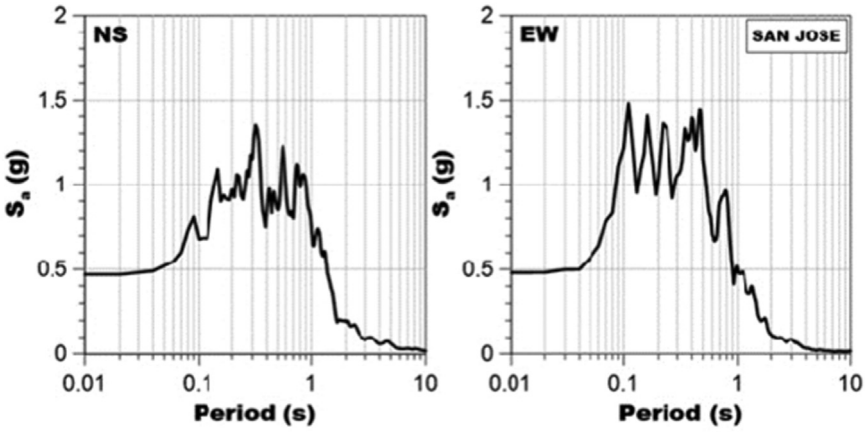

Fig. 14. Pseudo-acceleration response spectra computed from recorded accelerations of the Maule Earthquake in San Jose station.

spectrum, the actual problem arises from a practical point of view, because the HVSR also does not show a predominant period. This could be as a limitation of the applicability of the HVSR to estimate the predominant period.

Fig. 15 shows four typical different shapes of HVSR obtained by means of ambient vibrations in Santiago [51]. Shape 1, commonly associated with soft soils, shows a clear peak that permits the identification of the predominant period of the site. Shape 2, associated with medium to soft soils, also shows a clear peak, but its amplitude is rather low, less than 3–4. Shapes 3 and 4 are basically flat, showing no amplification. These flat shapes of the HVSR are associated with very stiff soil deposits such as the Santiago gravel, with shear wave velocity greater than 700 m/s [52].

Therefore, it can be concluded that when a flat shape of the HVSR is obtained, the site corresponds to a stiff material, where the seismic amplification is reduced in comparison with others sites. This is an important practical fact, because it makes possible the identification of those sites that develop a low to moderate seismic response.

Therefore, it is possible to conclude that the use of the HVSR of ambient vibration measurements permits the evaluation of the predominant period of a site. When this procedure does not provide a value because the result is a flat plot, it means the analyzed ground is associated with a stiff site.

7. Equivalent shear wave velocity, $V_{S30\text{-}E}$

The current shear wave velocity of the upper 30 m, V_{S30}, corresponds to the shear wave velocity that reproduces the same propagation

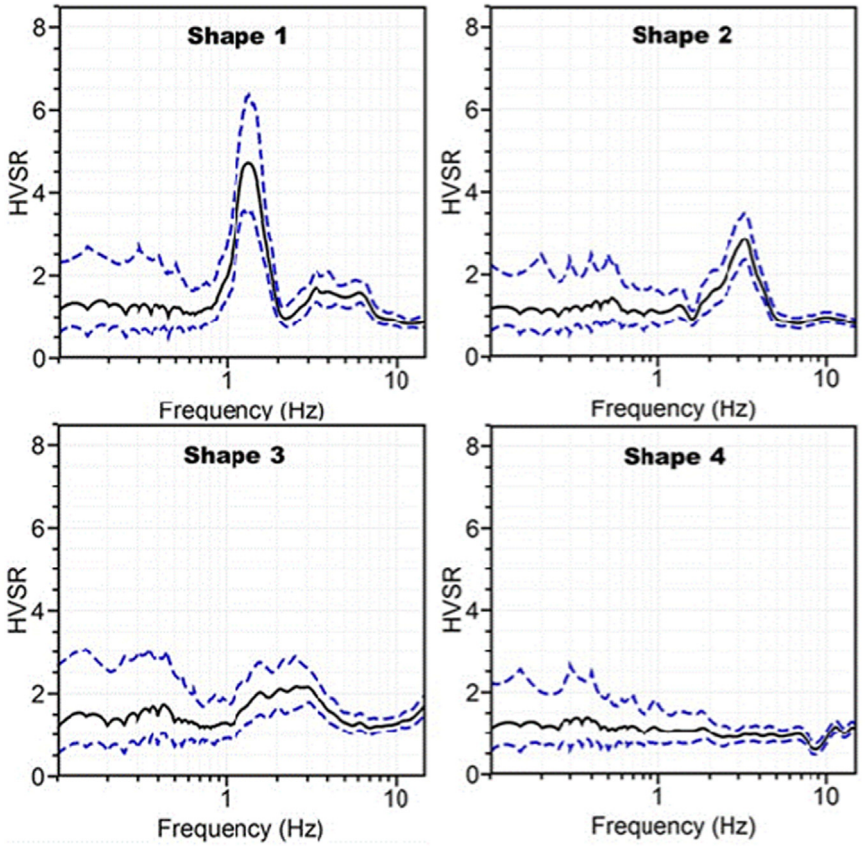

Fig. 15. Typical observed shapes of the HVSR.

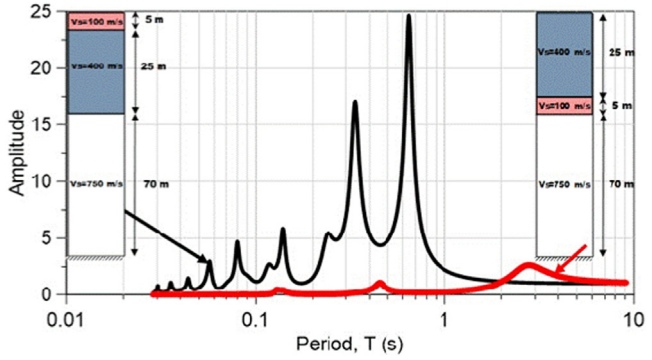

Fig. 16. Transfer functions of two soil profiles with identical V_{S30} but different location of a soft layer.

time of the actual upper 30 m of the ground. This implies that the sequence of different soil layers does not affect the value of V_{S30}. However, the seismic response at the ground surface can be strongly affected by the sequence of the soil layers. For example, Fig. 16 presents the transfer function base-surface of two stratigraphic profiles, with identical V_{S30} (267 m/s), both including a soft 5 m-thick layer with V_S = 100 m/s. In one profile the soft layer is on the surface, while in the other profile the soft layer is located at a depth of 25 m. It can be seen that when the soft layer is located below the layer of V_S = 400 m/s, it practically acts as a seismic isolator, while at the surface it amplifies the response due to the large impedance. This simple example shows that V_{S30} is not a good parameter because it does not capture the fundamental characteristics associated with the seismic soil response. To overcome this situation, it is proposed to use an equivalent shear wave velocity that reproduces the same stiffness of the actual top 30 m of the site. In other words, it is proposed to use a shear wave velocity that reproduces the same fundamental period of the isolated upper 30 m of the ground.

It important to remark that in this analysis exclusively the top 30 m of the soil deposit are considered. To evaluate the lateral stiffness of these upper 30 m, the numerical model consists of a rigid base with the 30 m of soils characterized by the shear wave velocity of each layer existing in these 30 m. Knowing the stratigraphy of the top 30 m of a site in terms of thickness and shear wave velocity of each layer, the theoretical fundamental period, $T_{F\text{-}30}$, of the isolated top 30 m, can be computed numerically, using for instance, the 1D equivalent linear analysis. Then, the evaluation of the equivalent shear wave velocity, $V_{S30\text{-}E}$, is straightforward using the well-known expression of the fundamental period of a single stratum of 30 m in thickness:

$$V_{S30-E} = \frac{120}{T_{F-30}} \tag{5}$$

The capability of $V_{S30\text{-}E}$ for assessing the seismic response of layered grounds has been checked by means of 1D analyses considering different complex soil stratigraphy. Three different soil layers in the upper 30 m of a rather deep site have been considered. Each layer has the same thickness of 10 m and shear wave velocities of 100, 250 and 400 m/s. Below 30 m, a soil with a shear wave velocity of 650 m/s and 50 m in thickness has been included. For six different combinations of the three upper soil layers, Fig. 17 shows the resulting theoretical transfer functions when the current V_{S30}, the proposed $V_{S30\text{-}E}$ and the actual layered soil structure, are used in the numerical analyses.

Regardless the sequence of these three layers, the conventional shear wave velocity of the top 30 m has the same value, V_{S30} = 182 m/s. However, for the sequences considered in this example, the values of $V_{S30\text{-}E}$ are different as summarized in Table 7, varying in the range of 114–242 m/s.

It can be observed that different order or sequence of the soil layers generates different lateral stiffness of the upper 30 m (fundamental period of these 30 m of soil deposit), and therefore, different values of $V_{S30\text{-}E}$, which can clearly modify the current site classification. For the first mode, the proposed equivalent shear wave velocity is in good agreement with the different transfer functions of each of the analyzed stratigraphy (Fig. 17).

8. Proposed seismic site classification

A fundamental observation is associated with the fact that during large or mega-earthquakes, very rigid soil deposits, such as rock outcrops, cemented soils or very dense gravels, have shown a significant reduction in the number of damaged structures, even cases of no damage have been reported on these type of sites. Conversely, soft soil deposits, as for example, the clayey material of Mexico City, or the bay mud of San Francisco, or the sandy soils of Valparaíso, have shown a dramatic number of damaged structures as well as fully collapsed ones. With this strong and repeated empirical evidence, the seismic site classification must be able to identify and group appropriately the different sites according to the expected similar seismic behavior.

The best seismic behavior has been observed in rock outcrops. Therefore, the best material in a site characterization has to be massive rock (Site Class A), which can be characterized simply by a shear wave velocity equal or greater than 800 m/s in the top 30 m.

Continuing, it is considered that soil deposits with a high stiffness are those with a fundamental period smaller than 0.3 s and a shear wave velocity greater than 500 m/s. Therefore, a Site Class B is proposed, with properties $V_{S30\text{-}E} > 500$ m/s and a predominant period obtained from HVSR, $T_{H/V} < 0.3$ s, or flat HVSR such as Shape 4 of Fig. 15.

Site Class A and Site Class B are associated with sites that generate the lowest seismic demand when a large earthquake hits an area. The corresponding design spectra must reflect this condition.

To consider stiff sites, it is important to keep in mind that very dense uncemented sandy soils, may in exceptional cases reach shear wave velocities close to 400 m/s at confining pressure less than 1 MPa. However, for the same level of pressure, common values of V_S for uncemented dense sandy soils are of the order 280 m/s. Therefore, a stiff site can be represented by shear wave velocities in the range of 300–500 m/s. In terms of fundamental period, a range between 0.3 and 0.5 s is suggested. Consequently, a Site Class C is proposed, with properties $V_{S30\text{-}E} > 300$ m/s and a predominant period obtained from HVSR, $T_{H/V} < 0.5$ s, or flat HVSR such as Shape 4 of Fig. 15.

The following Site Class D is associated with medium to low stiff soil deposits, which can be characterized by $V_{S30\text{-}E} > 180$ m/s and a predominant period obtained from HVSR, $T_{H/V} < 0.8$ s.

The softer classification corresponds to Site Class E, with $V_{S30\text{-}E} < 180$ m/s. It is necessary to mention that Site Class D and Site Class E are the most seismically demanding sites, and therefore, must be analyzed carefully. Table 8 summarizes the proposed site classification. Site Class F is also included in order to group those sites with peculiar geological-geotechnical conditions that require special analyses, such as liquefiable soil, peats, quick clays, collapsible soils, expansive soils and saline soils.

The main parameter to classify a site is the equivalent shear wave velocity of the upper 30 m of the site, $V_{S30\text{-}E}$. Then, the predominant period, $T_{H/V}$, is an additional parameter that has to be used to confirm the Site Class. If the required predominant period is not satisfied, then, the resulting Site Class is degraded to the next Site Class.

Fig. 18 shows the response spectra computed from the acceleration time histories recorded in two sites during the Maule Earthquake. The Concepción site consists of about 110 m of a sandy soil deposit with a shallow water table, whereas Peñalolen site consists of a non-saturated clayey soil of 24 m in thickness, below which dense gravel materials are encountered. The values of $V_{S30\text{-}E}$ obtained in Concepción and Peñalolen are 240 and 290 m/s, respectively. If shear wave velocities of the top 30 m were used alone, these sites should be classified as Site Class

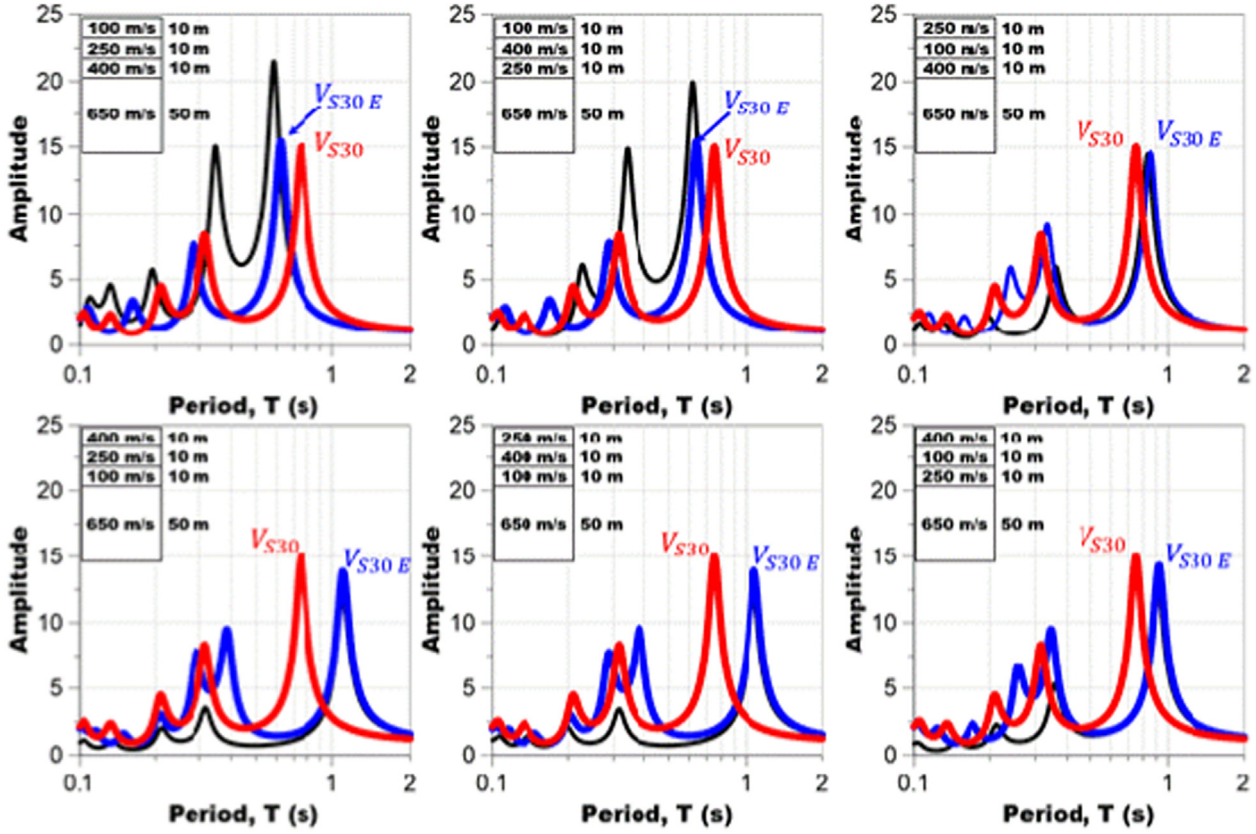

Fig. 17. Transfer functions considering in the upper 30 m: the current V_{S30} (in red), the proposed $V_{S30\text{-}E}$ (in blue) and the actual stratigraphy (* in black). (For interpretation of the references to color in this figure legend, the reader is referred to the web version of this article.).

Table 7
Variation of $V_{S30\text{-}E}$.

Sequencefrom top	$T_{F\text{-}30}$ (s)	$V_{S30\text{-}E}$ (m/s)
100–250–400	0.50	242
100–400–250	0.52	232
250–100–400	0.78	154
250–400–100	1.03	116
400–100–250	0.85	140
400–250–100	1.05	114

Table 8
Proposed seismic site classification.

Site Class	General description	$V_{S30\text{-}E}$ (m/s)	$T_{H/V}$ (s)
A	Rock	≥ 800	/
B	Very dense soils	≥ 500	< 0.30 (or flat)
C	Dense, firm soils	≥ 300	< 0.50 (or flat)
D	Medium-dense or medium-firm soils	≥ 180	< 0.80
E	Soft soils	< 180	/
F	Special soils	–	

D. However, when the predominant periods are considered, the site of Concepción ($T_{H/V}$ = 1.4 s) has to be modified, classifying as Site Class E. This site classification is in a good agreement with the actual observed spectra.

9. Concluding remarks

In spite of the advances in the field of earthquake engineering, economic losses left by large recent earthquakes are still considerable, far from any socio-economically satisfactory standard. Modern society is wanting not only life protection but is also demanding that buildings can be immediately occupied after a strong earthquake. Historically, seismic design has been oriented to provide resistance to the structure elements. However, this approach has been shown to be insufficient to guarantee successful seismic behavior of the structures. The new paradigm that would reduce the damage and losses resulting from an earthquake is the performance-based seismic design (PBSD). This design methodology allows engineers to design structures and non-structural components with a desired seismic performance for a

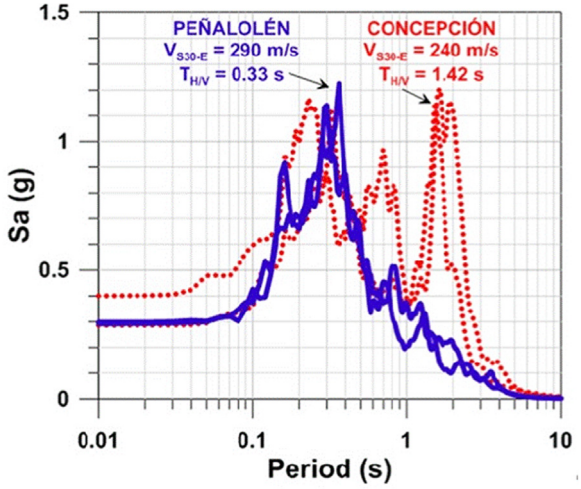

Fig. 18. Response spectra of Concepcion and Peñalolen sites, evaluated from acceleration records of Maule Earthquake.

specified level of hazard. Accordingly, seismic design has moved from resistance criteria to performance objectives that have to be satisfied by the structure during and after earthquakes. This design methodology requires a high standard in the different items that control the seismic analysis. One of the key factors is associated with the seismic loads, which are strongly dependent on the local ground conditions. The current Site Classifications used in different seismic countries have several flaws, which has identified and attempted to improve.

Acceleration time histories recorded during the Maule Earthquake (Mw = 8.8) and Illapel Earthquake (Mw = 8.3) were analyzed in terms of their pseudo-acceleration response spectra. To identify the predominant period of each station a complementary tool is proposed; the Arias Intensity Spectrum. It corresponds to the Arias Intensity of the acceleration response of each SDOF considering in the spectrum. This means that each considered frequency has associated a value of its Arias Intensity. This spectrum tends to exalt in a better way the predominant frequency, or period, of the signal.

The analyses of the available data permitted to confirm that the H/V spectral ratio obtained via ambient vibrations or micro-tremors, reproduces the predominant periods shown by the response spectra. Accordingly, it is proposed that the predominant period of the soil deposit be estimated via the H/V spectral ratio of ambient vibrations.

The equivalent shear wave velocity, $V_{S30\text{-}E}$, that reproduces the dynamic lateral stiffness of the upper 30 m of the ground is proposed as an alternative parameter to characterize the upper 30 m of a site. This parameter capture in a better way the fundamental characteristics of the seismic soil response.

An alternative seismic site classification has been proposed, which incorporates two important dynamic parameters of the ground: the equivalent shear wave velocity, $V_{S30\text{-}E}$, of the upper 30 m and the predominant period of the soil deposit. The main parameter to classify a site is $V_{S30\text{-}E}$. Then, the predominant period, $T_{H/V}$, is an additional parameter that has to be used to confirm the Site Class. If the required predominant period is not satisfied, then, the resulting Site Class is degraded to the next Site Class.

Acknowledgements

The author wants to acknowledge the valuable help of Dr. Laurence Wesley and Dr. Felipe Ochoa. The strong collaboration provided by the colleagues of CMGI Ltda., Javiera Gonzalez, Guillermo Valladares, Loreto Vergara and Gustavo Peters is also gratefully acknowledged.

References

[1] USGS. American Red Cross Multi-Disciplinary Team. Report on the 2010 Chilean Earthquake and Tsunami Response: U.S. Geological Survey Open-File Report 2011–1053. 2011; 2011. Available at: 〈https://pubs.usgs.gov/of/2011/1053/〉.
[2] Kajitani Y, Chang S, Tatano H. Economic impacts of the 2011 Tohoku-Oki Earthquake and Tsunami. Earthq Spectra 2013;29(S1):S457–78.
[3] Horspool N King A Lin S, Uma S. Damage and losses to residential buildings during the canterbury earthquake sequence. NZSEE Conference; 2016.
[4] Aon Benfield. Nepal earthquake event recap report; 2015. webpage at: impactforecasting.com.
[5] Senplades. Evaluación de los Costos de Reconstrucción Sismo en Ecuador Abril. Secretaría Nacional de Planificación y Desarrollo de Ecuador. (in Spanish); 2016.
[6] Cimellaro G. New trends on resiliency. In: Proceedings of the 16th world conference on earthquake engineering. Santiago, Chile; 2017.
[7] FEMA. Seismic performance assessment of buildings, Volume 1 – Methodology; 2012.
[8] Priestley MJN. Performance based seismic design. In: Proceedings of 12th WCEE; 2000.
[9] Dobry R, Borchert R, Crouse C, Idriss I, Joyner W, Martin G, Power M, Rinne E, Seed R. New site coefficients and site classification system used in recent building seismic code provisions. Earthq Spectra 2000;16(1):41–67.
[10] Pitilakis K Gazepis C Anastasiadis A. Design response spectra and soil classification for seismic code provisions. In: Proceedings of 13th WCEE. Vancouver, Canada; 2004.
[11] Ballore Montessusde. Seismic history of Southern Los Andes South of Parallel 16″ Cervantes Barcelona press. Santiago, Chile. (In Spanish); 1911.
[12] Watanabe T, Karzulovic J. The seismic ground motions of May 1960 in Chile (in Spanish). Anales de la Facultad de Ciencias Físicas y Matemáticas. Vol. 17. Universidad de Chile; 1960.
[13] Borcherdt R. Effect of local geology on ground motion near San Francisco Bay. Bull Seismol Soc Am 1970;60(1):29–61.
[14] Seed HB, Romo M, Sun J, Jaime A, Lysmer J. The Mexico Earthquake of September 19, 1985 – relationships between soil conditions and earthquake ground motions. Earthq Spectra 1988;4(4):687–729.
[15] Celebi M, Prince J, Dietel C, Onate M, Chavez G. The culprit in Mexico city amplification of motions. Earthq Spectra 1987;3:315–28.
[16] Singh S, Lermo J, Dominguez T, Ordaz M, Espinosa J, Mena E, Quaas R. The Mexico Earthquake of September 19, 1985 - a study of amplification of seismic waves in the Valley of Mexico with respect to a hill zone site. Earthq Spectra 1988;4:653–73.
[17] Borcherdt R, Gibbs J. Effects of local geological conditions in the San Francisco Bay region on ground motions and the intensities of the 1906 earthquake. Bull Seismol Soc Am 1976;66(2):467–500.
[18] Indirli M, Apablaza S. Heritage protection in Valparaiso (Chile): the “Mar Vasto” project. Rev Ing De Constr 2010;25(1).
[19] Rodriguez A, Gajardo C. La catástrofe del 16 de agosto de 1906 en la República de Chile. Natl Libr Chile 1906. [in Spanish].
[20] Henríquez H. El Terremoto de Agosto bajo el Punto de Vista Constructivo. (in Spanish); 1907.
[21] Seed HB, Ugas C, Lysmer J. Site-dependent spectra for earthquake-resistance design. Bull Seismol Soc Am 1976;66(1):221–43.
[22] Mohraz B. A study of earthquake response spectra for different geological conditions. Bull Seismol Soc Am 1976;66(3):915–35.
[23] Borcherdt R, Glassmoyer G. On the characteristics of local Geology and their influence on ground motions generated by the Loma Prieta earthquake in the San Francisco Bay region, California. Bull Seismol Soc Am 1992;82:603–41.
[24] Borcherdt R. Estimates of site-dependent response spectra for design (methodology and justification). Earthq Spectra 1994;10(4):617–53.
[25] ASCE/SEI 7-10. Minimum design loads for buildings and other structures. American Society of Civil Engineers. Third Printing, Revised commentary; 2013.
[26] Eurocode 8. Design of structures for earthquake resistance. European Committee for Standardization; 2004.
[27] DS 61. Decreto Supremo, Diseño Sísmico de Edificios. Diario Oficial de Chile. (In Spanish); 2011.
[28] Towhata I. Personal Communication; 2016.
[29] Bray J, Rodriguez-Marek A. Geotechnical site categories. In: Proceedings of the First PEER-PG&E Workshop on Seismic Reliability of Utility Lifelines. USA; 1997.
[30] Rodríguez-Marek A, Bray J, Abrahamson N. An empirical geotechnical seismic site response procedure. Earthq Spectra 2001;17(1).
[31] Stewart J, Liu A, Choi Y. Amplification factors for spectral acceleration in tectonically active regions. Bull Seismol Soc Am 2003;93(1):332–52.
[32] Zhao J, Irikura K, Zhang J, Fukushima Y, Somerville P, Asano A, et al. An Empirical site-classification method for strong-motion stations in Japan using H/V response spectral ratio. Bull Seismol Soc Am 2006;96(3):914–25.
[33] Gregor N, Abrahamson N, Atkinson G, Boore D, Bozorgnia Y, Campbell K, et al. Comparison of NGA-West2 GMPEs. Earthq Spectra 2014;30(3):1179–97.
[34] Hassani B, Atkinson G. Applicability of the site fundamental frequency as a VS30 Proxy for Central and Eastern North America. Bull Seismol Soc Am 2016;106(2). http://dx.doi.org/10.1785/0120150259.
[35] Kwak D, Stewart J, Mandokhail S, Park D. Supplementing VS30 with H/V spectral ratios for predicting site effects. Bull Seismol Soc Am 2017;107(5):2028–42.
[36] Verdugo R. Amplification phenomena observed in downhole array records generated on a subductive environment. Phys Earth Planet Inter 2009;175:63–77.
[37] Nakamura Y. A method for dynamic characteristics estimation of subsurface using microtremor on the ground surface. Q Rep. Railw Tech Res Inst (RTRI) 1989;30(1):25–33.
[38] Koller M, Chatelain J-L, Guiller B, Duval A-M, Atakan K, Lacave C, Bard PY. Practical user guidelines and software for the implementation of the H/V ratio technique: measuring conditions, processing method and results interpretation. 13WCEE. Vancouver, Canada; 2004.
[39] Konno K, Ohmachi T. Ground-motion characteristics estimated from spectral ratio between horizontal and vertical components of microtremor. Bull Seismol Soc Am 1998;88:228–41.
[40] Lachet C, Bard PY. Numerical and theoretical investigations on the possibilities and limitations of Nakamura's technique”. J Phys Earth 1994;42:377–97.
[41] Lermo J, Chávez-García J. Site effect evaluation using spectral ratios with only one station. Bull Seismol Soc Am 1993;83(5):1574–94.
[42] Pastén C. Seismic response of Santiago Basin (Master thesis). Department of Civil Engineering, University of Chile. (in Spanish); 2007.
[43] Verdugo R, Pastén C. Seismic source and its effect on site response observed in Chilean subductive environment. In: Proceedings of the 6th .international conference on case histories in geotechnical engineering. Arlington. USA; 2008.
[44] Verdugo R, Gonzalez J. Liquefaction-induced ground damages during the 2010. Soil Dyn Earthq Eng 2015;79:280–95.
[45] Barrientos S. Technical Report Illapel Earthquake. National Seismological Center, CSN. (in Spanish); 2015.
[46] Arias A. A measure of earthquake intensity. In: Hansen RJ, editor. Seismic design for nuclear power plants. MIT Press; 1970. p. 438–83.
[47] Kokusho T. Nonlinear site response and strain-dependent soil properties. Curr Sci 2004;87(10):1363–9.
[48] Noguchi S, Sasatani T. Quantification of degree of nonlinear site response. The 14WCEE. Beijing, China; 2008.
[49] Régnier J Cadet H, Bard PY. Impact of non-Linear soil behavior on site response amplitude. 16WCEE. Santiago, Chile; 2017.
[50] Choi Y, Stewart JP. Nonlinear site amplification as function of 30 m shear wave velocity. Earthq Spectra 2005;21:1–30.
[51] Vergara L, Verdugo R. Characteristics of the grounds with severely damaged buildings in the 27F earthquake. In: Proceedings of the IX Chilean congress of geotechnical engineering. Valdivia. (in Spanish); 2016.
[52] Pastén C, Sáez M, Ruiz S, Leyton F, Salomón J, Poli P. Deep characterization of the Santiago Basin using HVSR and cross-correlation of ambient seismic noise. Eng Geol 2016;201:57–66.